



# Lawrence Berkeley Laboratory

UNIVERSITY OF CALIFORNIA

## Materials & Molecular Research Division

LBL--20488

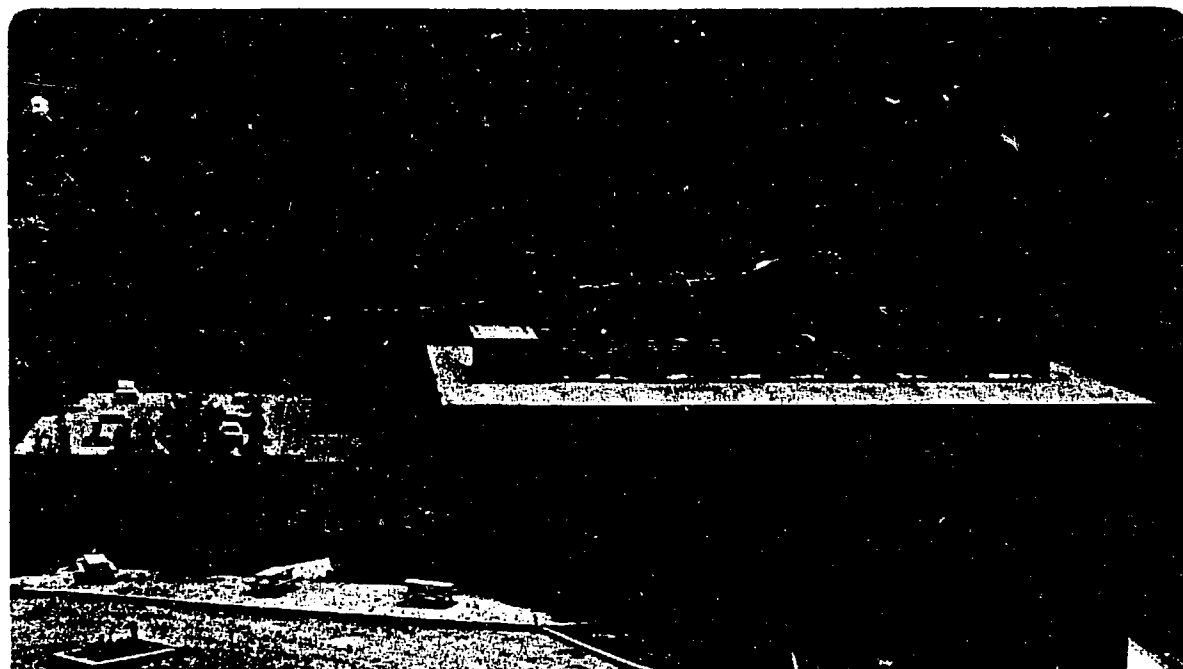
DE86 006273

Presented at the Frontiers of Quantum Chemistry,  
Los Alamos, NM, September 3-6, 1985

MOLECULAR PHYSICS AND CHEMISTRY APPLICATIONS OF  
QUANTUM MONTE CARLO

P.J. Reynolds, R.N. Barnett, B.L. Hammond,  
and W.A. Lester, Jr.

September 1985



Molecular Physics and Chemistry Applications of Quantum Monte Carlo<sup>1</sup>P. J. Reynolds, R. N. Barnett<sup>2</sup>, B. L. Hammond<sup>2</sup>, and W.A. Lester, Jr.<sup>2</sup>

Materials and Molecular Research Division,  
Lawrence Berkeley Laboratory,  
University of California,  
Berkeley, California 94720, U.S.A.

**Abstract.**

We discuss recent work with the diffusion quantum Monte Carlo (QMC) method in its application to molecular systems. The formal correspondence of the imaginary time Schrödinger equation to a diffusion equation allows one to calculate quantum mechanical expectation values as Monte Carlo averages over an ensemble of random walks. We report work on atomic and molecular total energies, as well as properties including electron affinities, binding energies, reaction barriers, and moments of the electronic charge distribution. A brief discussion is given on how standard QMC must be modified for calculating properties. Calculated energies and properties are presented for a number of molecular systems, including He, F, F<sup>-</sup>, H<sub>2</sub>, N, and N<sub>2</sub>. Recent progress in extending the basic QMC approach to the calculation of "analytic" (as opposed to finite-difference) derivatives of the energy is presented, together with an H<sub>2</sub> potential-energy curve obtained using analytic derivatives.

**Key Words:** diffusion quantum Monte Carlo, Schrödinger equation, fixed nodes, atomic properties, molecular properties, total energies, analytic energy derivatives, excited states, quadrupole moments, binding energies, electron affinities.

**DISCLAIMER**

This report was prepared as an account of work sponsored by an agency of the United States Government. Neither the United States Government nor any agency thereof, nor any of their employees, makes any warranty, express or implied, or assumes any legal liability or responsibility for the accuracy, completeness, or usefulness of any information, apparatus, product, or process disclosed, or represents that its use would not infringe privately owned rights. Reference herein to any specific commercial product, process, or service by trade name, trademark, manufacturer, or otherwise does not necessarily constitute or imply its endorsement, recommendation, or favoring by the United States Government or any agency thereof. The views and opinions of authors expressed herein do not necessarily state or reflect those of the United States Government or any agency thereof.

<sup>1</sup> This work was supported by the Director, Office of Energy Research, Office of Basic Energy Sciences, Chemical Sciences Division of the U. S. Department of Energy under contract number DE-AC03-76SF00098

<sup>2</sup> Also, Department of Chemistry, University of California, Berkeley, CA 94720

**MASTER**

JSL

## I. Introduction

In the past few years, quantum mechanical Monte Carlo (QMC) methods have begun to be applied in the domain of atomic and molecular physics<sup>(1-6)</sup>. Long in the realm of condensed-matter physics, and more recently nuclear and particle physics, Monte Carlo methods play an indispensable role in treating multi-dimensional, and hence many-body problems. For obtaining molecular properties, the Monte Carlo technique is now showing itself to be equally useful, providing an approach complementary to traditional *ab initio* electronic-structure calculations.

Atomic and molecular QMC applications have been primarily devoted to calculations of ground-state energies. Workers have focused on correlation energies<sup>(1,2)</sup> as well as on stationary points on potential-energy surfaces<sup>(3,4)</sup>. In these studies, total energies have been obtained to accuracies of better than 99.9%. Though impressive by most standards, an accuracy of 99.9% is only marginally useful for many chemical applications, in which one seeks very small differences of large numbers. Thus better algorithms and faster computers are still needed. In Section II we review the use of QMC in calculations of ground-state energies, and give an extension to excited states. Results are presented for a number of atomic and molecular species. Section III describes the calculation of other molecular properties, including the calculation of energy derivatives, which are useful in the study of potential-energy surfaces.

## II. QMC Energy Calculations

### *Theory*

The QMC method of obtaining energies of atomic and molecular systems has been described in detail elsewhere<sup>(1-8)</sup>. The key point to note here is that a simulation is performed in which an ensemble of random walks (the coordinates of which, at any given time, represent a configuration of the electrons) evolves to an equilibrium distribution.

At any time after equilibrium has been reached, the ensemble of configurations is a random sample drawn from the probability distribution  $f_{\infty}(\underline{R}) = \Psi_T(\underline{R})\hat{\phi}(\underline{R})$ , where the coordinate-vector  $\underline{R}$  is the multi-dimensional vector describing the full many-electron system. Here  $\Psi_T(\underline{R})$  is a simple trial wave function used for importance sampling<sup>(9)</sup>. The function  $\hat{\phi}(\underline{R})$  is the lowest-energy eigenfunction of the Schrödinger equation which is not orthogonal to  $\Psi_T$ . Convergence to the lowest-energy state results from an essential feature of the mapping of the Schrödinger equation into its diffusion equation analog--that time in these two equations differs by a factor of  $i$ . Thus, when a time-dependent molecular state vector is expanded in energy eigenfunctions multiplied by  $\exp(-iEt/\hbar)$ , in imaginary time one obtains a series in which only the lowest-energy term (i.e.  $\hat{\phi}$ ) survives at large  $t$ . If  $\Psi_T$  is orthogonal to the exact lowest-energy state, one projects out the ground state, and convergence will be to the next-lowest energy. In the fixed-node approximation<sup>(10)</sup>, which we use to handle the Fermion problem, the nodes of  $\Psi_T$  are imposed on the solution  $\hat{\phi}$ .

Although neither  $\hat{\phi}$  nor  $f_{\infty}$  is known analytically, one can nevertheless sample desired quantities from the equilibrium distribution  $f_{\infty}$ . Averages taken with respect to  $f_{\infty}$  are known as mixed averages. For example, sampling a quantity  $A$  in equilibrium gives (in the limit of large  $N$ ) the average

$$\langle A \rangle_{f_{\infty}} = \langle \Psi_T | A | \hat{\phi} \rangle, \quad (1)$$

where the Dirac notation being used has the normalization absorbed. The correct expectation value of  $A$ , for a state  $\hat{\phi}$ , is  $\langle \hat{\phi} | A | \hat{\phi} \rangle$ ; however, in computing any property for which  $\hat{\phi}$  is an eigenstate, there is no difference between these two averages. This follows since the eigenvalue can be taken out of the integral in Eq. 1. In particular, to compute the energy one samples the quantity  $E_L(\underline{R}) = \Psi_T^{-1}(\underline{R})H\Psi_T(\underline{R})$ . Then

$$\langle E \rangle_{f_{\infty}} = \langle \hat{\phi} | H | \Psi_T \rangle = \hat{E}_0, \quad (2)$$

where  $\hat{E}_0$  is defined by  $H\hat{\phi} = \hat{E}_0\hat{\phi}$ .

## Results

Table I reports the total energies obtained for a number of atomic and molecular species. These energies are compared with Hartree-Fock results, with the best variational calculations to date, and with exact or experimental values. QMC compares quite favorably with the other methods, generally performing better than the best of the other calculations.

When studying excited states of a given symmetry, such as the He states displayed in Table I, it is generally not possible to find a trial wave function exactly orthogonal to all the lower-energy states of that symmetry. This implies (cf. Eq. 2) that convergence will ultimately be to the lowest-energy state; however, the fixed-node approximation used to treat the Fermi problem is also of assistance in this context. In the fixed-node approximation, the nodes of  $\Psi_T$  are used to divide  $\underline{R}$ -space into distinct volume elements. The Schrödinger equation is solved separately in each of these elements. This results in a solution of the Schrödinger equation with added boundary conditions. Viewed this way, the Fermi problem is handled by forcing the generation of an antisymmetric state above the Bose ground state through the placement of nodes in the solution  $\hat{\phi}$ . In like manner, other excited states can be treated approximately by imposing additional nodes. The accuracy of the approximation will depend on how well these nodes are placed. Furthermore, if  $\Psi_T$  is not orthogonal to all lower energy states, the approximation is no longer variational.

Traditional *ab initio* methods generate excited-state wave functions which generally contain the correct number and dimensionality of nodal surfaces. Thus such wave functions are a good place to begin in choosing a trial wave function  $\Psi_T$ . In our work on the excited states of He, we have taken a sum of two Slater determinants in  $\Psi_T$  to obtain the required spatial symmetry. Although the result for the (1s2s)  $^1S$  state is not as accurate as that for the 1s3s state, our calculated energy is nevertheless within 0.66

kcal/mol of the experimental value. This is generally considered chemical accuracy.

### III. QMC Molecular Properties

#### *Energy-Related Quantities*

Table II reports the results obtained for a number of atomic and molecular properties. The first four columns are properties that are derived from the energy. Thus, for example, separate energy calculations of F and F<sup>-</sup> are performed, and the difference gives the electron affinity. Most of the properties give impressively close agreement with experimental results. The somewhat larger discrepancy in the binding energy of N<sub>2</sub> is probably attributable to the fixed-node approximation.

Another important quantity is the potential-energy surface of a molecule, which is obtained in the Born-Oppenheimer approximation from the solution of the electronic Schrödinger equation. Derivatives of the energy with respect to nuclear coordinates are very useful in accurately determining potential-energy surfaces including critical points, e.g. transition states and barriers, as well as in determining equilibrium geometries <sup>(11)</sup>, and (by finite difference or higher analytic derivatives) in obtaining vibrational frequencies <sup>(12)</sup>. While advances over the past decade in conventional *ab initio* approaches allow the direct calculation of derivatives, only finite difference approaches have been implemented in QMC <sup>(13)</sup>. In principle there is no reason for this limitation. The energy derivative with respect to a nuclear coordinate  $\rho$ , can be written <sup>(14)</sup>

$$\begin{aligned} \frac{d \langle E \rangle_{I_\infty}}{d \rho} = & \left\langle \frac{\partial E_L}{\partial \rho} \right\rangle_{I_\infty} + \left\langle \frac{1}{\hat{\phi}} \frac{\partial \hat{\phi}}{\partial \rho} E_L \right\rangle_{I_\infty} - \left\langle \frac{1}{\hat{\phi}} \frac{\partial \hat{\phi}}{\partial \rho} \right\rangle_{I_\infty} \langle E_L \rangle_{I_\infty} \\ & + \left\langle \frac{1}{\Psi_T} \frac{\partial \Psi_T}{\partial \rho} E_L \right\rangle_{I_\infty} - \left\langle \frac{1}{\Psi_T} \frac{\partial \Psi_T}{\partial \rho} \right\rangle_{I_\infty} \langle E_L \rangle_{I_\infty}. \quad (3) \end{aligned}$$

Although  $\hat{\phi}^{-1} \partial \hat{\phi} / \partial \rho$  is unknown, it is possible to sample it. The other terms in Eq. 3 may be evaluated straight-forwardly during the QMC simulation. Rather than sampling  $\hat{\phi}^{-1} \partial \hat{\phi} / \partial \rho$ , as a first approximation we take  $\hat{\phi}^{-1} \partial \hat{\phi} / \partial \rho = \Psi_T^{-1} \partial \Psi_T / \partial \rho$ . This turns out to

be a good approximation even when  $\Psi_T$  is only of moderate accuracy.

Using this approach, we have performed calculations on  $H_2$  at several nuclear separations. Combining the QMC energies and derivatives at only four points leads to the curve shown in Figure 1. Compared to the exact curve obtained by Kolos and Wolniewicz<sup>(15)</sup>, our error is less than the thickness of the line.

### *Other Expectation Values*

For expectation values of quantities whose operators do not commute with  $H$ , the mixed average of Eq. (1) is only approximate. One suspects that the mixed average is in some sense "half-way" between the exact expectation value (with respect to  $\hat{\phi}$ ) and the variational expectation value, taken with respect to the trial wave function, i.e.  $\langle \Psi_T | A | \Psi_T \rangle$ . Taken literally, this implies that  $\langle \hat{\phi} | A | \hat{\phi} \rangle = 2\langle \Psi_T | A | \hat{\phi} \rangle - \langle \Psi_T | A | \Psi_T \rangle$ . This result can be formalized to first order in the difference  $\delta = \hat{\phi} - \Psi_T$ <sup>(8,14)</sup>. It is, however, difficult to know how significant it is to drop terms of order  $\delta^2$ . Thus, it is desirable to be able to sample exactly from the distribution  $|\hat{\phi}|^2$ . This can be done, though it entails some changes in the usual QMC algorithm.

To sample from the distribution  $|\hat{\phi}|^2$ , the distribution  $f_\infty$  must be weighted locally by  $\hat{\phi}(\underline{R})/\Psi_T(\underline{R})$ . This quantity is essentially the asymptotic number of survivors of the local configuration  $\underline{R}$ <sup>(16)</sup>. Thus, algorithmically, one must follow each configuration into the future before computing any averages. As a walk progresses, one must not only keep track of its immediate descendants (which is easy), but also the descendants of its descendants for a large number of generations. At first sight, this seems to be a very difficult task. But the problem can be greatly simplified by visualizing the branching process in time as a "tree." The tree expands vertically in time,  $t$ , and, as it branches, expands horizontally (or sometimes visualized as azimuthally) in the  $\theta$  direction. The location of each configuration in the tree is uniquely described by the pair of

values  $(\theta, t)$ . In addition, we require that all branches emanating from  $(\theta, t)$  have  $\theta$  in the range from  $\theta$  to  $\theta + \Delta$ . No other branches are allowed within this range. This is accomplished through a proper choice of  $\Delta$ . Following this procedure, the required weighting factor for configuration  $i$  at some later time is simply the number of configurations which lie between  $\theta_i$  and  $\theta_i + \Delta_i$  at this later time. Hence the only work required is to assign each configuration, at each step in the walk, a value of  $\theta$  and  $\Delta$  by the above scheme, and at a later (asymptotic) time to count the number of walks falling in a particular range. This relatively simple algorithm thus allows one to compute properties from the correct probability distribution. A more detailed discussion will be published elsewhere<sup>(17)</sup>.

Our results using the above algorithm to compute the electric quadrupole moment of  $H_2$  (see Table II), show that excellent results may be obtained with QMC by sampling from the  $|\hat{\phi}|^2$  distribution. On the other hand, the  $N_2$  results use the approximate formula, and are also of high quality. Thus it appears that one may not always need to use the more complicated algorithm.

In summary, QMC is a powerful and accurate method of calculating energies and properties of atomic and molecular systems. The results presented in Tables I and II and Fig. 1 demonstrate its utility. In this paper we have demonstrated several new capabilities of the method. We have also pointed to areas requiring further development, such as exactly orthogonal excited-state trial functions, and other approaches to excited states. Interestingly, in our approach the fixed-node approximation, which is the only obstacle to calculating exact ground-state energies, is the very tool needed in the calculation of excited-state energies. We have also shown that QMC can be employed to calculate *smooth* potential-energy surfaces, and near basis-set independent properties. These capabilities make QMC an attractive method to use for atomic and molecular calculations.



## Acknowledgements

We thank C. Dateo and R. M. Grimes for helpful comments on the manuscript, and also for discussions during the course of this work. Some of the work described here was supported by a grant from the Office of Naval Research.

## References.

1. P. J. Reynolds, D. M. Ceperley, B. J. Alder, and W. A. Lester, Jr., *J. Chem. Phys.* 77, 5593 (1982).
2. J. W. Moskowitz, K. E. Schmidt, M. A. Lee, and M. H. Kalos, *J. Chem. Phys.* 77, 349 (1982).
3. P. J. Reynolds, R. N. Barnett, and W. A. Lester, Jr., *Int. J. Quant. Chem. Symp.* 18, 709 (1984); F. Mentch and J. Anderson, *J. Chem. Phys.* 80, 2675 (1984); R. N. Barnett, P. J. Reynolds, and W. A. Lester, Jr., *J. Chem. Phys.*, 82, 2700 (1985).
4. D. M. Ceperley and B. J. Alder, *J. Chem. Phys.* 81, 5833 (1984)
5. P. J. Reynolds, M. Dupuis, and W. A. Lester, Jr., *J. Chem. Phys.* 82, 1983 (1985).
6. See also the article by K. E. Schmidt in this issue.
7. M. H. Kalos, *Phys. Rev.* 128, 1791 (1962); *J. Comp. Phys.* 1, 257 (1967); M. H. Kalos, D. Levesque, and L. Verlet, *Phys. Rev. A* 9, 2178 (1974); D. M. Ceperley in *Recent Progress in Many-Body Theories*, edited by J. G. Zabolitzky, M. de Llano, M. Fortes, and J. W. Clark (Springer-Verlag, Berlin, 1981).
8. D. M. Ceperley and M. H. Kalos in *Monte Carlo Methods in Statistical Physics*, K. Binder, ed. (Springer-Verlag, Berlin, 1979).
9. J. M. Hammersley and D. C. Handscomb, *Monte Carlo Methods*, (Methuen, London, 1964).
10. D. M. Ceperley and B. J. Alder, *Phys. Rev. Lett.* 45, 566 (1980);
11. P. Pulay, in *Modern Theoretical Chemistry*, Vol. 4, H. F. Schaefer III, ed. (Plenum, New York, 1977); M. Dupuis and H. F. King, *J. Chem. Phys.* 68, 3998 (1978).
12. P. Saxe, Y. Yamaguchi, and H. F. Schaefer III, *J. Chem. Phys.* 77, 5647 (1982).
13. B. Holmer and D. M. Ceperley, *private communication*; B. Wells, P. J. Reynolds, and W. A. Lester, Jr., *unpublished*; B. H. Wells, *Chem. Phys. Lett.* 115, 89 (1985).
14. P. J. Reynolds, R. N. Barnett, B. L. Hammond, R. M. Grimes, and W. A. Lester, Jr., "Quantum Chemistry by Quantum Monte Carlo: Beyond Ground-State Energy Calculations," *Int. J. Quant. Chem.* *in press*.
15. W. Kolos and L. Wolniewicz, *J. Chem. Phys.* 43, 2429 (1965).
16. M. H. Kalos, *Phys. Rev. A* 2, 250 (1970).
17. R. N. Barnett, P. J. Reynolds, and W. A. Lester, Jr., "Molecular Properties by Quantum Monte Carlo" *in preparation*.
18. Z. Ritter and R. Pauncz, *J. Chem. Phys.* 32, 1820 (1960).

19. From Ref. 18, where this result is attributed to the experimental work of C. E. Moore, Natl. Bur. Standards Circ. No. 467, I (1949).
20. W. Kolos and C. C. J. Roothaan, Rev. Mod. Phys. 32, 219 (1960).
21. B. Liu, J. Chem. Phys. 58, 1925 (1973).
22. E. Clementi and C. Roetti, At. Data Nucl. Data Tables 14, 177 (1974).
23. P. E. M. Siegbahn, Int. J. Quant. Chem. 23, 1869 (1983).
24. A. Veillard and E. Clementi, J. Chem. Phys. 49, 2415 (1968).
25. P. A. Christiansen and E. A. McCullough, Jr., J. Chem. Phys. 67, 1877 (1977).
26. F. Grimaldi, J. Chem. Phys. 43, S59 (1965).
27. F. Sasaki and M. Yoshimine, Phys. Rev. A 9, 17, 26 (1974).
28. E. Clementi and A. D. McLean, Phys. Rev. 133 A, 419 (1964).
29. S. Fraga, J. Karwowski, K. M. S. Saxena, *Handbook of Atomic Data* (Elsevier, Amsterdam, 1976).
30. B. H. Botch and T. H. Dunning, Jr., J. Chem. Phys. 76, 6046 (1982).
31. R. N. Barnett, P. J. Reynolds, and W. A. Lester, Jr., "Electron Affinity of Fluorine: A Quantum Monte Carlo Study" J. Chem. Phys. *submitted*.
32. H. Hotop and W. C. Lineberger, J. Phys. Chem. Ref. Data 4, 539 (1975).
33. A. Lofthus and P. H. Krupenie, J. Phys. Chem. Ref. Data 6, 113 (1977).
34. B. Liu, J. Chem. Phys. 80, 581 (1984).
35. D. Feller, L. E. McMurchie, W. T. Borden, and E. R. Davidson, J. Chem. Phys. 77, 6134 (1982); P. Saxe, H. F. Schaefer III, and N. C. Handy, J. Phys. Chem. 85, 745 (1981).
36. H.-J. Werner and E.-A. Reinsch, J. Chem. Phys. 76, 3144 (1982).
37. A. R. W. McKellar, P. R. Bunker, T. J. Sears, K. M. Evenson, R. J. Saykally, and S. R. Langhoff, J. Chem. Phys. 79, 5251 (1983).
38. A. D. McLean and M. Yoshimine, J. Chem. Phys. 45, 3676 (1966).
39. F. P. Billingsley II and M. Krauss, J. Chem. Phys. 60, 2767 (1974).

## Table Captions

**Table I.** Energies (in hartrees) for a number of atomic and molecular species. QMC energies for the first two excited  $^1S$  states of He, as well as the ground states of  $H_2$ , N,  $N_2$ , F, and  $F^-$  are compared with Hartree-Fock results, with the best variational calculations to date, and with exact or experimental results.

**Table II.** Atomic and molecular properties for a number of species. Again QMC is compared with Hartree-Fock, with the best variational results, and with exact or experimental values. In general, QMC agrees well with the best calculations performed, as well as with experiment. The properties treated are the electron affinity  $A$  of F, the binding energy  $E_B$  of  $N_2$ , the barrier to chemical reaction for  $H + H_2$  exchange, the singlet-triplet energy difference  $T_e$  in  $CH_2$ , and the electric quadrupole moment  $Q$  of  $H_2$  and  $N_2$ .

## Figure Captions

**Figure 1.** QMC potential-energy curve for  $H_2$ . A Hermite polynomial fit to the energy and derivatives provides a curve indistinguishable from exact to the resolution of the line. A polynomial fit to the energy alone gives oscillatory behavior. The statistical error bars on the points are smaller than the points themselves.

Table I.

Method	He (1s2s)	He (1s3s)	H <sub>2</sub>	N	N <sub>2</sub>	F	F <sup>-</sup>
Hartree-Fock	-2.143 07 <sup>a</sup>	-2.060 36 <sup>a</sup>	-1.133 6 <sup>c</sup>	-54.400 9 <sup>g</sup>	-108.993 9 <sup>j</sup>	-99.409 3 <sup>g</sup>	-99.459 4 <sup>g</sup>
Best Variational	-2.143 07 <sup>a</sup>	-2.060 36 <sup>a</sup>	-1.173 7 <sup>d</sup>	-54.513 3 <sup>h</sup>	-109.365 8 <sup>h</sup>	-99.716 6 <sup>m</sup>	-99.831 2 <sup>m</sup>
QMC	-2.144 93(7)	-2.061 19(7)	-1.174 5(8) <sup>e</sup>	-54.576 5(12)	-109.483 5(37)	-99.700 5(21)	-99.827 3(34)
Experimental or Exact	-2.145 99 <sup>b</sup>	-2.061 28 <sup>b</sup>	-1.174 47 <sup>f</sup>	-54.589 5 <sup>i</sup>	-109.535 <sup>k</sup>	-99.731 3 <sup>i</sup>	-99.857(3) <sup>n</sup>

<sup>a</sup> Ref. 18.

<sup>b</sup> Ref. 19.

<sup>c</sup> Ref. 20.

<sup>d</sup> Ref. 21. This is the best configuration interaction calculation for H<sub>2</sub>. Explicitly correlated variational results for H<sub>2</sub> are essentially exact. See Ref. 15.

<sup>e</sup> Ref. 1.

<sup>f</sup> From the essentially exact calculation in Ref. 15.

<sup>g</sup> Ref. 22.

<sup>h</sup> Ref. 23.

<sup>i</sup> From experimental results corrected for relativistic effects in Ref. 24. Ref. 27 corrects an error in the sign of the Lamb shift, resulting in the energy given here.

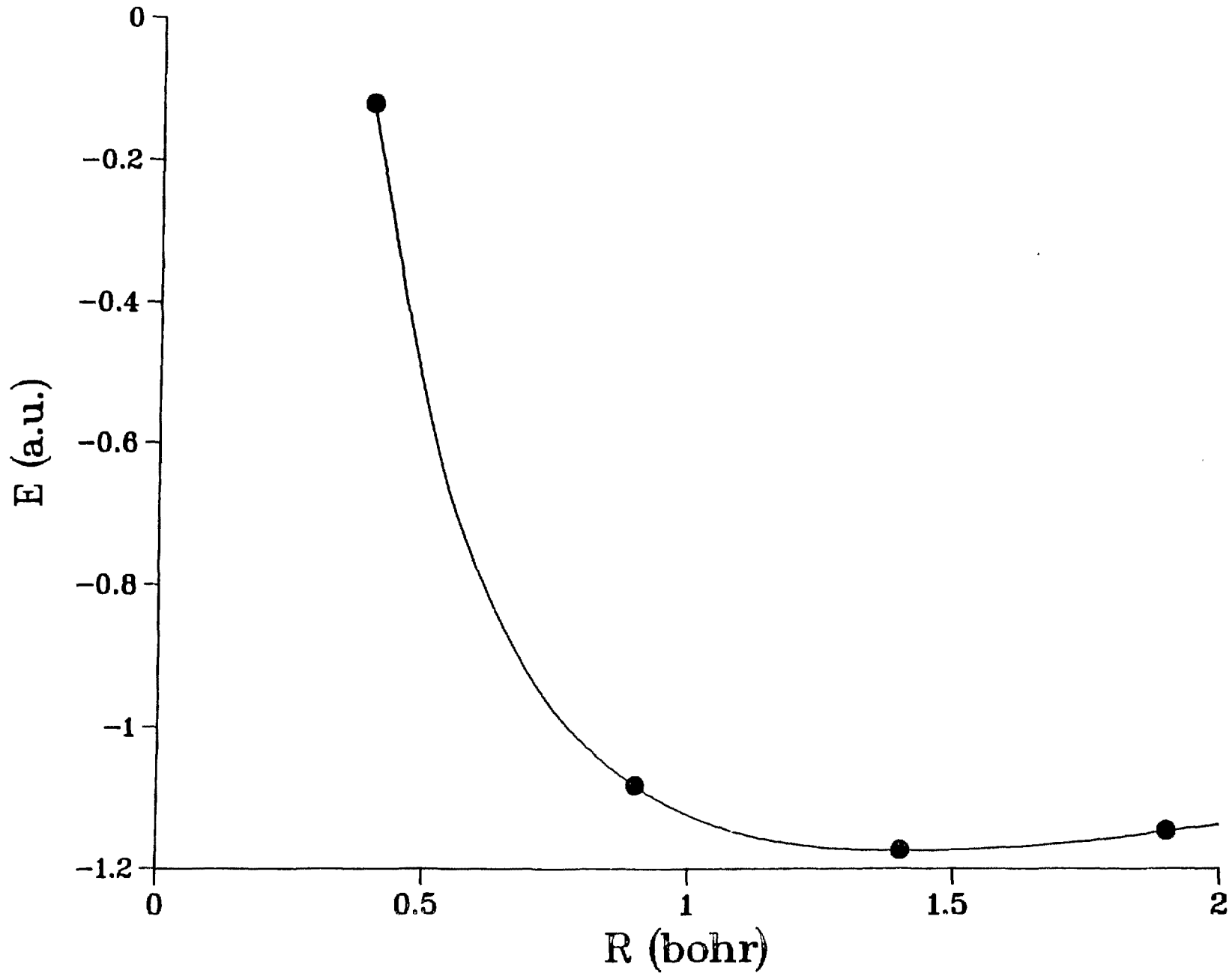
<sup>j</sup> Ref. 25.

<sup>k</sup> Ref. 26.

<sup>m</sup> Ref. 27.

<sup>n</sup> From experimental results corrected for relativistic effects in Ref. 28.

# Hydrogen Molecule Potential Curve



This report was done with support from the Department of Energy. Any conclusions or opinions expressed in this report represent solely those of the author(s) and not necessarily those of The Regents of the University of California, the Lawrence Berkeley Laboratory or the Department of Energy.

Reference to a company or product name does not imply approval or recommendation of the product by the University of California or the U.S. Department of Energy to the exclusion of others that may be suitable.